Shift in the LHC Higgs diphoton mass peak from interference with background

Stephen P. Martin

Shift in the LHC Higgs diphoton mass peak from interference with background

Stephen P. Martin

Department of Physics, Northern Illinois University, DeKalb IL 60115 and

Fermi National Accelerator Laboratory, P.O. Box 500, Batavia IL 60510

The Higgs diphoton amplitude from gluon fusion at the LHC interferes with the continuum background induced by quark loops. I investigate the effect of this interference on the position of the diphoton invariant mass peak used to help determine the Higgs mass. At leading order, the interference shifts the peak towards lower mass by an amount of order 150 MeV or more, with the precise value dependent on the methods used to analyze and fit the data.

The ATLAS and CMS collaborations at the CERN Large Hadron Collider (LHC) have recently announced the discovery of a resonance with production rates and decay branching ratios that are at least approximately consistent with the Standard Model Higgs scalar boson [1, 2]. In this paper, this resonance will be assumed to be indeed the Standard Model Higgs H. The detailed properties of H, including measurements of its spin and CP quantum numbers, mass, production cross-sections in various channels, and branching ratios will be the focus of long-term experimental and theoretical investigations. The mass of H is currently estimated to be $125.3 \pm 0.4(\text{stat}) \pm 0.5(\text{syst})$ GeV by CMS and $126.0 \pm 0.4(\text{stat}) \pm 0.4(\text{syst})$ by ATLAS. After the accumulation of much more data, the experimental uncertainty in the mass may be reduced to perhaps [3] 0.1 GeV, motivating efforts to reduce theoretical sources of error as much as is possible.

The purpose of this note is to point out the effect of signal-background interference on the determination of the Higgs mass from data in the diphoton final state. The largest production cross-section for H is from gluon-gluon fusion $gg \to H$ [4], through loop diagrams mediated by quarks, with the top quark providing by far the biggest contribution. A tremendous effort has been expended in computing higher order corrections, including next-to-next-to-leading order in QCD [5–11], next-to-leading order in electroweak couplings [12–14], and next-to-next-to-leading logs in soft gluon resummation [15, 16]; for reviews see [17–20]. The rare but clean decay $H \to \gamma\gamma$ [21–26] is also mediated by loop diagrams. The excellent electromagnetic energy resolution of the ATLAS and CMS detectors makes this channel, along with $H \to ZZ^{(*)} \to \ell^+\ell^-\ell'^+\ell'^-$, one of the two best ways to determine M_H. The largest contribution to the $H \to \gamma\gamma$ amplitude comes from the W loop, with a subdominant contribution of the opposite sign coming from the top quark. (In this paper, the loop effects of t, b, c quarks and the τ lepton, including their mass dependences, are included in the H production and decay amplitudes.) The complete process $gg \to H \to \gamma\gamma$ is therefore of 2-loop order. It can interfere with the continuum background process $gg \to \gamma\gamma$, which is mediated by quarks beginning at one-loop order.

Dicus and Willenbrock found [27] that the effect of the interference on the total $\gamma\gamma$ rate is very small at leading order because the interference involving the real parts of the amplitudes is odd in $\hat{s}$ (the invariant squared mass of the parton-level process) around M_H, while the imaginary part of the continuum $gg \to \gamma\gamma$ amplitude has a quark mass suppression for the helicity combinations

that can interfere with Higgs exchange. Dixon and Siu have shown [28] that the most important interference effect on the cross-section instead comes from the imaginary part of the continuum amplitude $gg \to \gamma\gamma$ at 2-loops [29] (which, for the $++ \to ++$ and $-- \to --$ polarization configurations, does not have the mass suppression for the complex phase found at 1-loop order), and that it is destructive and typically of order 2-5% depending on the scattering angle. In the present paper, I consider the orthogonal issue of the shift in the position of the diphoton peak invariant mass distribution. I will show that the leading-order effect of the interference results in a downward shift of the $M_{\gamma\gamma}$ peak, of order 150 MeV or more, compared to the result one would obtain when interference is ignored. The precise magnitude of this shift will depend on the method used to analyze and fit the data. Other studies of the effects of the interference of the Higgs with backgrounds include [30–32] for $gg \to H \to W^+W^-$, [32–34] for $gg \to H \to ZZ$, and [35] for $\gamma\gamma \to H \to b\bar{b}$ at a photon collider.

In making a precise determination of the Higgs mass, one must first choose a prescription to define it. Consider the renormalized propagator for H,

$$\frac{i}{\hat{s} - m_H^2 - \Pi_H(\hat{s})} = \frac{iF_H(\hat{s})}{\hat{s} - M_H^2 + iM_H\Gamma_H}, \tag{1}$$

where m_H is the tree-level mass and Π_H is the 1PI self-energy function, and $F_H(\hat{s})$ is a function that is slowly varying and satisfies $F_H \approx 1$ in the resonance region. The complex pole mass $M_H^2 - iM_H\Gamma_H$ is a gauge-invariant physical observable, with Γ_H the width of the Higgs, and will be used in the following to define the mass M_H. In the following, I will ignore the variation in F_H from 1 for simplicity; it would have only a very small effect on the considerations below for $M_H \sim 125$ GeV.

The leading order matrix element for $gg \to \gamma\gamma$ including both non-resonant and Higgs resonant amplitudes can be written as

$$\mathcal{M} = -\delta^{ab}\delta_{\lambda_1\lambda_2}\delta_{\lambda_3\lambda_4}\frac{A_{ggH}A_{\gamma\gamma H}}{\hat{s} - M_H^2 + iM_H\Gamma_H} + \delta^{ab}4\alpha\alpha_S \sum_{q=u,d,s,c,b,t} e_q^2 M_{\lambda_1\lambda_2\lambda_3\lambda_4}^q, \tag{2}$$

where $a, b = 1, \ldots, 8$ are $SU(3)_c$ adjoint representation indices for the gluons, and the circular polarizations labels $\pm$ are λ_1, λ_2 for the incoming gluons and λ_3, λ_4 for the outgoing photons. The 1-loop amplitudes for H coupling to gluons and to photons are

$$A_{ggH} = -\frac{\alpha_S}{8\sqrt{2}\pi v}\hat{s}\sum_{q=t,b,c} F_{1/2}(4m_q^2/\hat{s}), \tag{3}$$

$$A_{\gamma\gamma H} = -\frac{\alpha}{4\sqrt{2}\pi v}\hat{s}\left[F_1(4m_W^2/\hat{s}) + \sum_{f=t,b,c,\tau} N_c^f e_f^2 F_{1/2}(4m_f^2/\hat{s})\right], \tag{4}$$

where $v = 174$ GeV is the Higgs vacuum expectation value, and $N_c^f = 3$ (1) for $f =$ quarks (leptons) with electric charge e_f and mass m_f, and

$$F_1(x) = 2 + 3x[1 + (2 - x)f(x)], \tag{5}$$

$$F_{1/2}(x) = -2x[1 + (1-x)f(x)], \tag{6}$$

$$f(x) = \begin{cases} [\arcsin(\sqrt{1/x})]^2, & x \geq 1 \quad \text{(for } t, W), \\ -\frac{1}{4}\left[\ln\left(\frac{1+\sqrt{1-x}}{1-\sqrt{1-x}}\right) - i\pi\right]^2, & x \leq 1 \quad \text{(for } b, c, \tau). \end{cases} \tag{7}$$

The 1-loop matrix elements $M^q_{\lambda_1\lambda_2\lambda_3\lambda_4}$ mediated by quarks q are the same as found in $\gamma\gamma \to \gamma\gamma$ scattering [36], and are used here in the normalization and sign convention such that, when $m_q^2 \ll \hat{s}$, the polarization configurations that can give a non-zero interference with the Higgs-mediated amplitudes are:

$$M^q_{++--} = M^q_{--++} = 1, \tag{8}$$

$$M^q_{++++} = M^q_{----} = -1 + z\ln\left(\frac{1+z}{1-z}\right) - \frac{1+z^2}{4}\left[\ln^2\left(\frac{1+z}{1-z}\right) + \pi^2\right], \tag{9}$$

where $z = \cos\theta_{\text{CM}}$, with θ_{CM} the scattering angle in the diphoton center-of-momentum (CM) frame. Note that in this light quark limit, these amplitudes are real, while the polarizations that have non-trivial complex phases at 1-loop do not interfere with the H-mediated amplitude. In the following the u, d, s quarks are treated as massless and the full mass dependence of t, b, c quarks is included, using the formulas in [37, 38].

The contributions to the LHC diphoton production cross-section at leading order, in excess of the pure continuum background, can then be written as

$$\frac{d^2\sigma_{pp\to\gamma\gamma}}{d(\sqrt{\hat{s}})\,dz} = \frac{G(\hat{s})}{128\pi\sqrt{\hat{s}}D(\hat{s})}(N_H + N_{\text{int,Re}} + N_{\text{int,Im}}) \tag{10}$$

where

$$N_H = |A_{ggH}A_{\gamma\gamma H}|^2, \tag{11}$$

$$N_{\text{int,Re}} = -(\hat{s} - M_H)2\text{Re}[A_{ggH}A_{\gamma\gamma H}A^*_{gg\gamma\gamma}], \tag{12}$$

$$N_{\text{int,Im}} = -M_H\Gamma_H 2\text{Im}[A_{ggH}A_{\gamma\gamma H}A^*_{gg\gamma\gamma}], \tag{13}$$

for the Higgs and real and imaginary interference contributions. Here

$$A_{gg\gamma\gamma} = 2\alpha_S\alpha\sum_q e_q^2(M^q_{++++} + M^q_{++--}), \tag{14}$$

and

$$G(\hat{s}) = \int_{\hat{s}/s}^1 \frac{dx}{sx}g(x)g(\hat{s}/sx) \tag{15}$$

is the gluon-gluon luminosity function, and

$$D(\hat{s}) = (\hat{s} - M_H^2)^2 + M_H^2 \Gamma_H^2. \tag{16}$$

The numerical results below use $M_H = 125$ GeV and $\Gamma_H = 4.2$ MeV for purposes of presentation, even though the current experimental indications are for a slightly heavier H. The running $\overline{\text{MS}}$ fermion masses at $Q = M_H$ are taken to be $m_t = 168.2$ GeV, $m_b = 2.78$ GeV, $m_c = 0.72$ GeV, $m_\tau = 1.744$ GeV, and $\alpha = 1/127.5$. The gluon distribution function $g(x)$ and strong coupling $\alpha_S(Q)$ are taken from the MSTW2008 NLO set [39], with $Q^2 = \hat{s}$. Because the focus here is on the shift in the diphoton mass peak, the very small imaginary interference term in eq. (13) and its 2-loop counterpart discussed in [28] will be neglected here, since they are small and affect the overall size but not the shape of the invariant mass distribution. Numerical results will be shown for the 2012 run energy $\sqrt{s} = 8$ TeV, but the results on the shape (as opposed to the size) of the $M_{\gamma\gamma}$ distribution turn out to be nearly independent of the LHC beam energy at leading order. This is because the $\sqrt{s}$ dependence enters only through $G(\hat{s})$, which appears in front of both N_H and $N_{\text{int,Re}}$ in eq. (10).

In the leading order calculation given here, changes in the choices of renormalization and factorization scale only affect the size of the diphoton distribution but not its shape. This is again because the factorization scale at leading order enters only through $G(\hat{s})$ which is common to both N_H and $N_{\text{int,Re}}$, and also because both the continuum and resonance amplitudes are proportional to $\alpha \alpha_S$. However, one might expect a potentially large change from including genuine next-to-leading order effects (beyond the scope of the present paper), since the K-factors for both continuum and resonance diphoton production are known to be large.

The factor of $\hat{s} - M_H^2$ in $N_{\text{int,Re}}$ is odd about the Higgs peak, making its contribution to the total cross-section negligible when $\hat{s}$ is integrated over [27, 28]. However, the same factor implies a slight excess for $M_{\gamma\gamma} = \sqrt{\hat{s}}$ below M_H and a slight deficit above, therefore pushing the peak to lower $M_{\gamma\gamma}$ than it would be if interference were absent. This is shown first in the case without any experimental resolution effects for the photons, in Figure 1. The distribution shown is obtained from the real interference term in eq. (12), plugged in to eq. (10), after integrating over $-1 < z < 1$ and dividing by 2 for identical photons. The distribution shows a sharp peak and dip near $M_{\gamma\gamma} = M_H - \Gamma_H/2$ and $M_H + \Gamma_H/2$ respectively, but there are also long tails due to the Breit-Wigner shape. [Using a different prescription for the width in the Breit-Wigner lineshape, such as the running-width prescription with $D(\hat{s}) = (\hat{s} - M_H^2)^2 + \hat{s}[\Gamma_H(\hat{s})]^2$, does not significantly affect the results, because for a light Higgs boson the width term is only important very close to the resonance peak where the width term is nearly constant.]

At the LHC, the photon energies are smeared by detector effects, in ways that differ between the two experiments. A detailed treatment of these effects is beyond the scope of this paper, but as an approximation, Figure 2 shows the same interference as in Figure 1, but now convoluted with some representative Gaussian[†] functions with mass resolution widths $\sigma_{\text{MR}} = 1.3, 1.5, 1.7, 2.0$ and

---

[†] In the real experiments, the invariant mass responses are not Gaussian, depend on photon conversions, and are different in different parts of the detectors. Therefore, the results shown below should be qualitatively valid but not quantitatively precise.
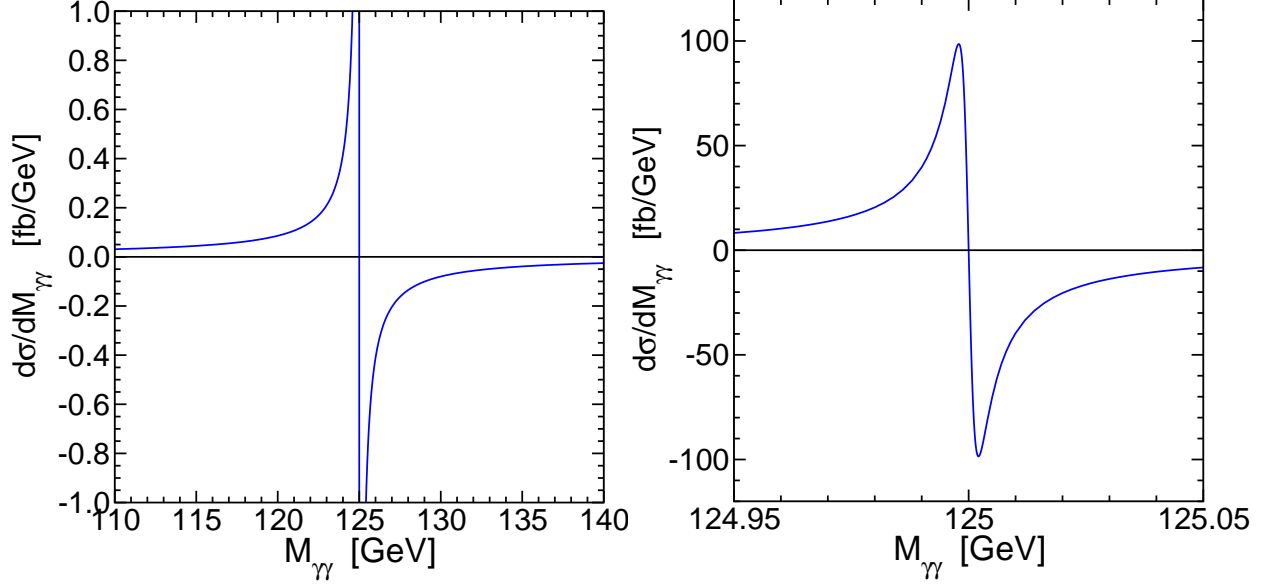
FIG. 1: The distribution of diphoton invariant masses from the real interference term in eq. (12), as a function of $M_{\gamma\gamma} = \sqrt{\hat{s}}$, from eq. (10), before including experimental resolution effects. The right panel is a close-up of the left panel, showing the maximum and minimum near $M_{\gamma\gamma} = M_H \pm \Gamma_H/2$.
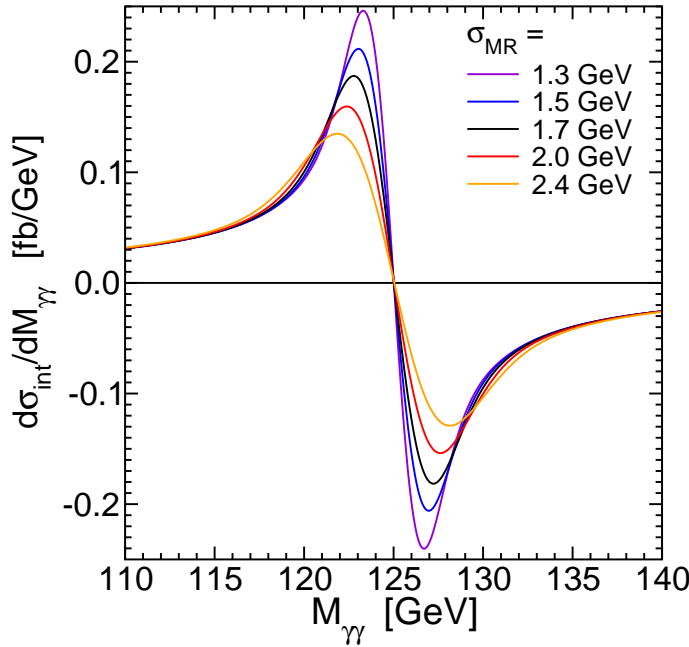

FIG. 2: The distribution of diphoton invariant masses from the real interference, as in Figure 1, but now smeared by various Gaussian mass resolutions with widths σ_{MR}.

2.4 GeV. This has the effect of reducing the peak and dip in the interference, and moving their points of maximal deviations from 0 much farther from M_H.

To obtain the size of the shift in the Higgs peak diphoton distribution, one can now combine the interference contribution with the non-interference contribution from eqs. (10) and (11). The results are shown in Figure 3 for the case of a Gaussian mass resolution $\sigma_{\mathrm{MR}} = 1.7$ GeV. The distribution obtained including the interference effect is shifted slightly to the left of the distribution obtained neglecting the interference. In order to quantify the magnitude of the shift, it will be necessary to specify the precise method used to fit the signal; this is again beyond the scope of the present
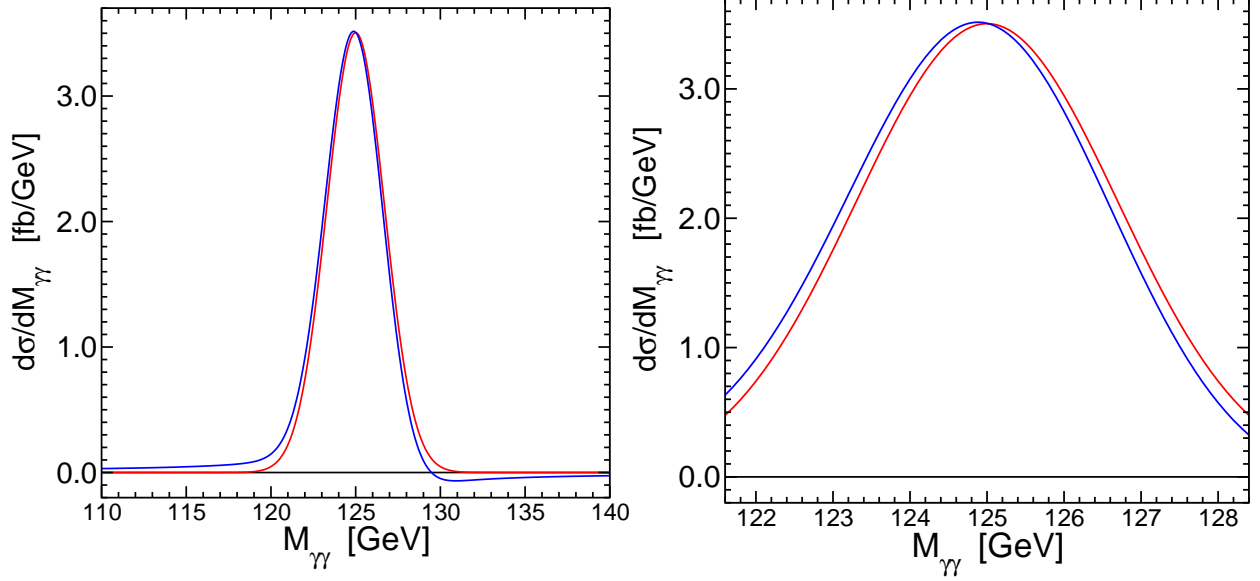
FIG. 3: Diphoton invariant mass distributions with a Gaussian mass resolution of width $\sigma_{\mathrm{MR}} = 1.7$ GeV. In each panel, the right (red) curve includes only the Higgs contribution without interference, and the left (blue) curve also includes the interference contribution from Figure 2. The right panel is a close-up of the left panel.

paper. The background levels are subject to significant higher order corrections [40–44], and in practice are obtained by the experimental collaborations using a sideband analysis of fitting to the falling background shape away from the Higgs peak. This fitting of the lineshape to background plus signal will be affected by the slight surplus (deficit) of events below (above) M_H, depending on exactly how the fit is done.

One simplistic way to estimate the shift is to take a mass window $|M_{\gamma\gamma} - M_{\mathrm{peak}}| < \delta$, where M_{peak} is the invariant mass at the maximum of the distribution, and δ is supposed to be large enough to include most of the excess events over background in the peak, and then compute

$$N_\delta = \int_{M_{\mathrm{peak}}-\delta}^{M_{\mathrm{peak}}+\delta} dM_{\gamma\gamma} \frac{d\sigma}{dM_{\gamma\gamma}}, \tag{17}$$

$$\langle M_{\gamma\gamma} \rangle_\delta = \frac{1}{N_\delta} \int_{M_{\mathrm{peak}}-\delta}^{M_{\mathrm{peak}}+\delta} dM_{\gamma\gamma} \, M_{\gamma\gamma} \, \frac{d\sigma}{dM_{\gamma\gamma}}. \tag{18}$$

Now

$$\Delta M_{\gamma\gamma} \equiv \langle M_{\gamma\gamma} \rangle_{\delta,\,\mathrm{total}} - \langle M_{\gamma\gamma} \rangle_{\delta,\,\mathrm{no\ interference}} \tag{19}$$

is a theoretical measure of the shift due to including the interference. For small δ ($\lesssim 1$ GeV), $\Delta M_{\gamma\gamma}$ is essentially just the shift in the maximum point of the distribution after subtracting background, which does not correspond to an experimentally well-measured quantity. However, one can see from Figure 3 that including a wider window, which should be more similar to the methods used to determine M_H by the experimental collaborations, will give a larger shift. In fact, the magnitude of the shift $\Delta M_{\gamma\gamma}$ actually grows approximately linearly with δ for all $\delta \gtrsim 2\sigma_{\mathrm{MR}}$, due to the long
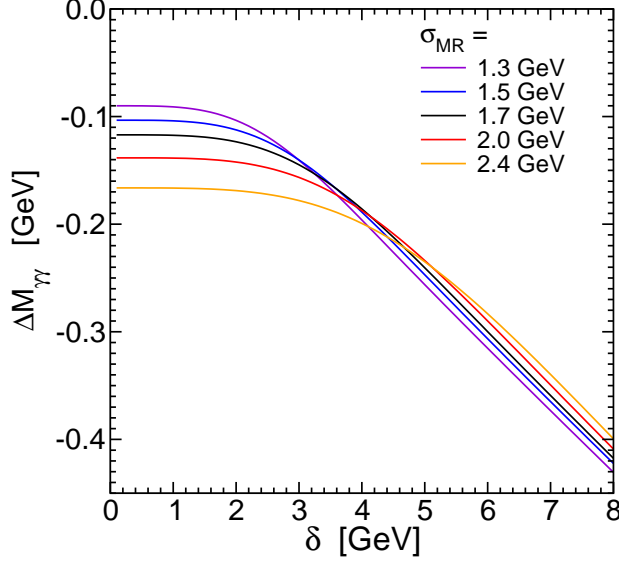
FIG. 4: The shift in the diphoton invariant mass distribution due to interference with the continuum background, using the measure of eqs. (17)-(19), for various assumed values of the mass resolution Gaussian width σ_{MR}.

positive (negative) tail at lower (higher) $M_{\gamma\gamma}$. This is shown in Figure 4, where $\Delta M_{\gamma\gamma}$ is given as a function of δ, for various values of the Gaussian mass resolution σ_{MR}. Because a Gaussian mass resolution is assumed here for simplicity, one finds $\langle M_{\gamma\gamma}\rangle_{\delta,\,\mathrm{no\ interference}} = M_H$ to very high precision, but $\langle M_{\gamma\gamma}\rangle_{\delta,\,\mathrm{total}}$ is increasingly smaller as δ is increased. If one takes a value like $\delta = 4$ GeV as indicative, since this is large enough to include most of the signal events, then from Figure 4 the shift is about -185 MeV, with not much sensitivity to the assumed mass resolution. However, even a moderately larger value of $\delta = 5$ GeV would increase the typical shift to about -240 MeV.

The results so far are based on total cross-sections, but experimental cuts and efficiencies favor scattering into the central regions of the detectors. In the CM frame, the non-interference part of the signal is isotropic, but the interference is peaked at large $|z| = |\cos\theta_{\mathrm{CM}}|$, as can be seen from eqs. (8), (9), (12), (14) and graphed in the left panel of Figure 5. The way this angular distribution would translate into the effects of a cut on $\eta = -\ln[\tan(\theta_{\mathrm{lab}}/2)]$ is shown in the right panel of Figure 5. Here I show the ratio of acceptances $R = (\sigma_{\mathrm{cut}}^{\mathrm{int}}/\sigma_{\mathrm{total}}^{\mathrm{int}})/(\sigma_{\mathrm{cut}}^{H}/\sigma_{\mathrm{total}}^{H})$ as a function of η_{max}, where "int" refers to the Higgs-continuum interference part from eq. (12) and "H" to the Higgs contribution without interference from eq. (11), and "cut" means $|\eta| < \eta_{\mathrm{max}}$ for both photons, while "total" means no cut on η. A simple cut on η does not translate into experimental reality, as the ATLAS Higgs analysis is sensitive to $|\eta| < 2.37$ except for $1.37 < |\eta| < 1.52$, and CMS to $|\eta| < 2.5$ except for $1.44 < |\eta| < 1.57$, but with efficiencies that vary over those ranges. Both experiments also have cuts on the photon p_T's, but the effect of this cannot be treated well by the present leading-order analysis. Furthermore, higher order corrections that have been neglected here could enhance or suppress the interference part relative to the non-interference part. To illustrate the possible effects of these considerations, Figure 6 depicts the impact on the shift $\Delta M_{\gamma\gamma}$ of a relative suppression of the interference part of the cross-section by a factor of r. This shows that the effect of such a suppression is to decrease the shift in the $M_{\gamma\gamma}$ peak by approximately the same factor r. For $r = 0.8$, the shift $\Delta M_{\gamma\gamma}$ found for $\delta = 4$ GeV would be reduced to about 150 MeV, although larger values are possible if the signal-background fitting procedure effectively corresponds to larger δ.
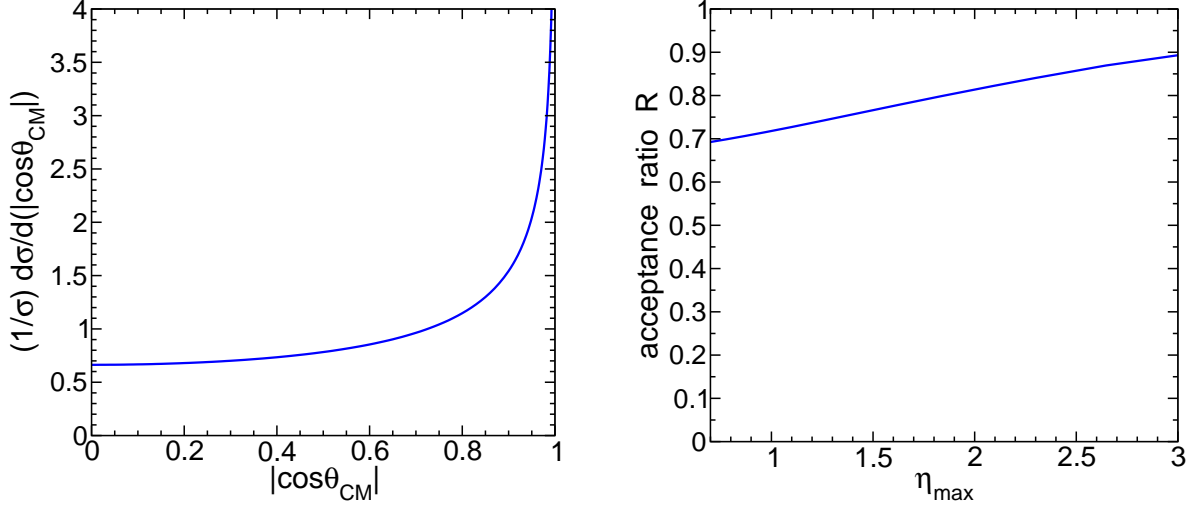
FIG. 5: Angular distributions for the diphoton Higgs signal-background interference. In the left panel, the shape of the interference contribution $(1/\sigma_{\text{int}})d\sigma_{\text{int}}/d(|\cos\theta_{\text{CM}}|)$, where θ_{CM} is the diphoton center-of-mass scattering angle. In the right panel, the ratio of the acceptances $R = (\sigma_{\text{cut}}^{\text{int}}/\sigma_{\text{total}}^{\text{int}})/(\sigma_{\text{cut}}^{H}/\sigma_{\text{total}}^{H})$, where "int" refers to the Higgs-continuum interference part from eq. (12) and "H" to the Higgs contribution without interference from eq. (11), and "cut" means $|\eta| < \eta_{\text{max}}$ for both photons, while "total" means no cut on η.
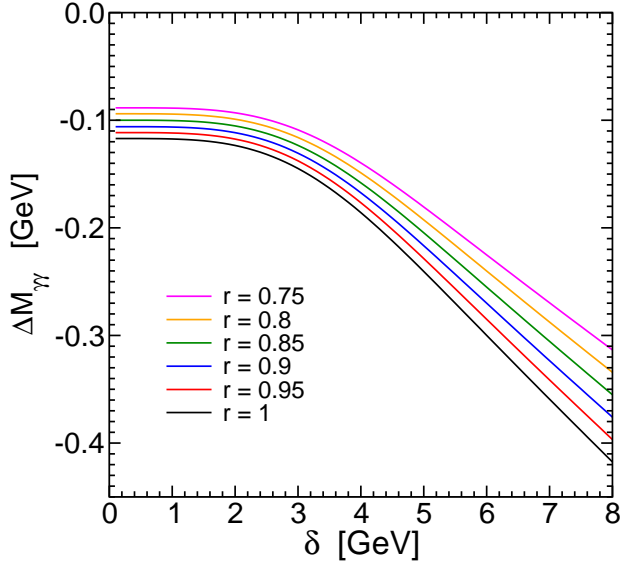

FIG. 6: The shift in the diphoton invariant mass distribution due to the interference effect, using the measure of eqs. (17)-(19) as in Figure 4, but for a fixed mass resolution $\sigma_{\text{MR}} = 1.7$ GeV, with the interference part of the total cross-section reduced by various factors r.

The measure of the mass shift used above is neither appropriate nor practical for use with real data, and does not correspond precisely to the techniques used by the experimental collaborations. However, the real lesson is that for a high precision determination of M_H, it will be necessary to fit to a signal lineshape that includes the interference effects. The leading-order estimates of this paper indicate that the interference shifts the Higgs diphoton mass distribution lower by an amount of order 150 MeV compared to the expectation based on neglecting interference, depending on the method used to fit the data. It would be useful to extend this analysis to include higher-order contributions and realistic experimental cuts. Although the shift is small, it is not negligible compared to the eventual precision that we may hope to obtain in the future, and to the last significant digit being reported by the experimental collaborations for M_H even now.

[1] G. Aad *et al.* [The ATLAS Collaboration], "Observation of a new particle in the search for the Standard Model Higgs boson with the ATLAS detector at the LHC," arXiv:1207.7214 [hep-ex], "Observation of an Excess of Events in the Search for the Standard Model Higgs boson with the ATLAS detector at the LHC", ATLAS-CONF-2012-093, July 7, 2012; "Observation of an excess of events in the search for the Standard Model Higgs boson in the gamma-gamma channel with the ATLAS detector", ATLAS-CONF-2012-091, July 6, 2012; "Observation of an excess of events in the search for the Standard Model Higgs boson in the $H \to ZZ^{(*)} \to 4l$ channel with the ATLAS detector" ATLAS-CONF-2012-092, July 5, 2012; "Observation of an Excess of Events in the Search for the Standard Model Higgs Boson in the $H \to WW \to l\nu l\nu$ Channel with the ATLAS Detector", ATLAS-CONF-2012-098, July 18, 2012.

[2] S. Chatrchyan *et al.* [The CMS Collaboration], "Observation of a new boson at a mass of 125 GeV with the CMS experiment at the LHC," arXiv:1207.7235 [hep-ex], "Observation of a new boson with a mass near 125 GeV", CMS-PAS-HIG-12-020, July 9, 2012; "Evidence for a new state decaying into two photons in the search for the standard model Higgs boson in pp collisions", CMS-PAS-HIG-12-015, July 8, 2012; "Evidence for a new state in the search for the standard model Higgs boson in the H to ZZ to 4 leptons channel in pp collisions at sqrt(s) = 7 and 8 TeV", CMS-PAS-HIG-12-016, July 9, 2012.

[3] "ATLAS: Detector and physics performance technical design report. Volume 2," CERN-LHCC-99-15.

[4] H. M. Georgi, S. L. Glashow, M. E. Machacek and D. V. Nanopoulos, "Higgs Bosons from Two Gluon Annihilation in Proton Proton Collisions," Phys. Rev. Lett. **40**, 692 (1978).

[5] S. Dawson, "Radiative corrections to Higgs boson production," Nucl. Phys. B **359**, 283 (1991).

[6] A. Djouadi, M. Spira and P. M. Zerwas, "Production of Higgs bosons in proton colliders: QCD corrections," Phys. Lett. B **264**, 440 (1991).

[7] M. Spira, A. Djouadi, D. Graudenz and P. M. Zerwas, "Higgs boson production at the LHC," Nucl. Phys. B **453**, 17 (1995) [hep-ph/9504378].

[8] R. V. Harlander and W. B. Kilgore, "Next-to-next-to-leading order Higgs production at hadron colliders," Phys. Rev. Lett. **88**, 201801 (2002) [hep-ph/0201206].

[9] C. Anastasiou and K. Melnikov, "Higgs boson production at hadron colliders in NNLO QCD," Nucl. Phys. B **646**, 220 (2002) [hep-ph/0207004].

[10] V. Ravindran, J. Smith and W. L. van Neerven, "NNLO corrections to the total cross-section for Higgs boson production in hadron hadron collisions," Nucl. Phys. B **665**, 325 (2003) [hep-ph/0302135].

[11] C. Anastasiou, K. Melnikov and F. Petriello, "Fully differential Higgs boson production and the di-photon signal through next-to-next-to-leading order," Nucl. Phys. B **724**, 197 (2005) [hep-ph/0501130].

[12] U. Aglietti, R. Bonciani, G. Degrassi and A. Vicini, Phys. Lett. B **595**, 432 (2004) [hep-ph/0404071].

[13] S. Actis, G. Passarino, C. Sturm and S. Uccirati, "NLO Electroweak Corrections to Higgs Boson Production at Hadron Colliders," Phys. Lett. B **670**, 12 (2008) [arXiv:0809.1301 [hep-ph]].

[14] C. Anastasiou, R. Boughezal and F. Petriello, "Mixed QCD-electroweak corrections to Higgs boson production in gluon fusion," JHEP **0904**, 003 (2009) [arXiv:0811.3458 [hep-ph]].

[15] S. Catani, D. de Florian, M. Grazzini and P. Nason, "Soft gluon resummation for Higgs boson production at hadron colliders," JHEP **0307**, 028 (2003) [hep-ph/0306211].

[16] D. de Florian, G. Ferrera, M. Grazzini and D. Tommasini, "Transverse-momentum resummation: Higgs boson production at the Tevatron and the LHC," JHEP **1111**, 064 (2011) [arXiv:1109.2109 [hep-ph]].

[17] D. de Florian and M. Grazzini, "Higgs production through gluon fusion: Updated cross sections at the Tevatron and the LHC," Phys. Lett. B **674**, 291 (2009) [arXiv:0901.2427 [hep-ph]].

[18] S. Dittmaier *et al.* [LHC Higgs Cross Section Working Group Collaboration], "Handbook of LHC Higgs Cross Sections: 1. Inclusive Observables," arXiv:1101.0593 [hep-ph].

[19] S. Dittmaier, *et al.*, "Handbook of LHC Higgs Cross Sections: 2. Differential Distributions,"

arXiv:1201.3084 [hep-ph].

[20] C. Anastasiou, S. Buehler, F. Herzog and A. Lazopoulos, "Inclusive Higgs boson cross-section for the LHC at 8 TeV," JHEP **1204**, 004 (2012) [arXiv:1202.3638 [hep-ph]].

[21] J. R. Ellis, M. K. Gaillard and D. V. Nanopoulos, "A Phenomenological Profile of the Higgs Boson," Nucl. Phys. B **106**, 292 (1976).

[22] M. A. Shifman, A. I. Vainshtein, M. B. Voloshin and V. I. Zakharov, "Low-Energy Theorems for Higgs Boson Couplings to Photons," Sov. J. Nucl. Phys. **30**, 711 (1979) [Yad. Fiz. **30**, 1368 (1979)].

[23] J. F. Gunion, P. Kalyniak, M. Soldate and P. Galison, Phys. Rev. D **34**, 101 (1986).

[24] R. K. Ellis, I. Hinchliffe, M. Soldate and J. J. van der Bij, Nucl. Phys. B **297**, 221 (1988).

[25] J. F. Gunion, G. L. Kane and J. Wudka, Nucl. Phys. B **299**, 231 (1988).

[26] A. Djouadi, J. Kalinowski and M. Spira, Comput. Phys. Commun. **108**, 56 (1998) [hep-ph/9704448].

[27] D.A. Dicus and S.S.D. Willenbrock, "Photon Pair Production And The Intermediate Mass Higgs Boson," Phys. Rev. D **37**, 1801 (1988).

[28] L.J. Dixon and M.S. Siu, "Resonance continuum interference in the diphoton Higgs signal at the LHC," Phys. Rev. Lett. **90**, 252001 (2003) [hep-ph/0302233].

[29] Z. Bern, A. De Freitas and L.J. Dixon, "Two loop amplitudes for gluon fusion into two photons," JHEP **0109**, 037 (2001) [hep-ph/0109078].

[30] T. Binoth, M. Ciccolini, N. Kauer and M. Kramer, "Gluon-induced W-boson pair production at the LHC," JHEP **0612**, 046 (2006) [hep-ph/0611170].

[31] J.M. Campbell, R.K. Ellis and C. Williams, "Gluon-Gluon Contributions to W+ W- Production and Higgs Interference Effects," JHEP **1110**, 005 (2011) [arXiv:1107.5569 [hep-ph]].

[32] N. Kauer and G. Passarino, "Inadequacy of zero-width approximation for a light Higgs boson signal," arXiv:1206.4803 [hep-ph].

[33] E. W. N. Glover and J. J. van der Bij, "Vector Boson Pair Production Via Gluon Fusion," Phys. Lett. B **219**, 488 (1989). E. W. N. Glover and J. J. van der Bij, "Z Boson Pair Production Via Gluon Fusion," Nucl. Phys. B **321**, 561 (1989).

[34] G. Passarino, "Higgs Interference Effects in $gg \to ZZ$ and their Uncertainty," arXiv:1206.3824 [hep-ph].

[35] L.J. Dixon and Y. Sofianatos, "Resonance-Continuum Interference in Light Higgs Boson Production at a Photon Collider," Phys. Rev. D **79**, 033002 (2009) [arXiv:0812.3712 [hep-ph]].

[36] R. Karplus and M. Neuman, "The scattering of light by light," Phys. Rev. **83**, 776 (1951).

[37] V. Costantini, B. De Tollis and G. Pistoni, "Nonlinear effects in quantum electrodynamics," Nuovo Cim. A **2**, 733 (1971).

[38] B.L. Combridge, "Consequences Of The Photon-Gluon Induced Couplings Of QCD," Nucl. Phys. B **174**, 243 (1980).

[39] A. D. Martin, W. J. Stirling, R. S. Thorne and G. Watt, "Parton distributions for the LHC," Eur. Phys. J. C **63**, 189 (2009) [arXiv:0901.0002 [hep-ph]].

[40] T. Binoth, J. P. Guillet, E. Pilon and M. Werlen, "A Full next-to-leading order study of direct photon pair production in hadronic collisions," Eur. Phys. J. C **16**, 311 (2000) [hep-ph/9911340].

[41] Z. Bern, L.J. Dixon and C. Schmidt, "Isolating a light Higgs boson from the diphoton background at the CERN LHC," Phys. Rev. D **66**, 074018 (2002) [hep-ph/0206194].

[42] J. M. Campbell, R. K. Ellis and C. Williams, "Vector boson pair production at the LHC," JHEP **1107**, 018 (2011) [arXiv:1105.0020 [hep-ph]].

[43] C. Balazs, E. L. Berger, P. M. Nadolsky and C. -P. Yuan, "All-orders resummation for diphoton production at hadron colliders," Phys. Lett. B **637**, 235 (2006) [hep-ph/0603037]. P. M. Nadolsky, C. Balazs, E. L. Berger and C. -P. Yuan, "Gluon-gluon contributions to the production of continuum diphoton pairs at hadron colliders," Phys. Rev. D **76**, 013008 (2007) [hep-ph/0702003 [HEP-PH]]. C. Balazs, E. L. Berger, P. M. Nadolsky and C. -P. Yuan, "Calculation of prompt diphoton production cross-sections at Tevatron and LHC energies," Phys. Rev. D **76**, 013009 (2007) [arXiv:0704.0001 [hep-ph]].

[44] S. Catani, L. Cieri, D. de Florian, G. Ferrera and M. Grazzini, "Diphoton production at hadron colliders: a fully-differential QCD calculation at NNLO," Phys. Rev. Lett. **108**, 072001 (2012) [arXiv:1110.2375 [hep-ph]].